JOURNAL OF MATERIALS SCIENCE 21 (1986) 3850–3858

Microstructural evaluation of rapidly solidified Al–Li–Be alloys

J. WADSWORTH, A. R. PELTON*, D. D. CROOKS, R. E. LEWIS, A. E. VIDOZ
*Lockheed Palo Alto Research Laboratory, Metallurgy Department, 3251 Hanover Street, Palo Alto, California 94304, USA and *Ames Research Laboratory, Ames, Iowa 50011, USA*

Aluminium–lithium–beryllium alloys are a group of low-density, high-modulus materials that potentially have technological importance in aerospace structures. In this paper, a series of such alloys has been produced using rapid solidification processing via melt spinning. The microstructures of the alloys have been investigated in the as-melt-spun condition, after consolidation and heat treatment to peak hardness, and after tensile testing in the heat-treated condition. In particular, changes in the size and distribution of primary beryllium particles and Al_3Li precipitates are described after consolidation and processing. The mechanical properties of the alloys in the heat-treated condition are also presented.

1. Introduction

The rationale for the development of ternary Al–Li–Be alloys has been presented recently by Lockheed scientists [1, 2]. It was shown that such alloys could have important applications for aerospace structures because of their high potential weight savings. The weight savings originate from the fact that both lithium and beryllium decrease the density of aluminium and at the same time increase the elastic modulus. In fact, lithium and beryllium are the only elements that significantly have both of these effects when added to aluminium. Recent studies of the various factors influencing weight savings in aerospace structures clearly emphasize the dominant importance of reduced density [2].

The production of wrought Al–Li–Be alloys by conventional ingot casting having useful engineering properties is not possible [1, 2]. This is because beryllium segregates in a coarse distribution upon freezing, and this results in poor ductility and toughness. Because of the extremely limited room temperature solubility of beryllium in aluminium, alloys based on the Al–Be system constitute an important case for the application of a rapid solidification processing (RSP) technique. At low temperature, although beryllium has only a small solid solubility in aluminium, 0.03 wt %, at increased temperatures (Fig. 1 of Wadsworth *et al.* [2]), it shows an increasing liquid solubility, reaching approximately 10% by weight at 1025° C. Therefore, it is possible to obtain by rapid solidification a microstructure in which the aluminium solid solution contain a high concentration of fine discrete particles (dispersoids) of beryllium. A fine dispersion of these particles can have at least three important effects upon the mechanical properties of the aluminium alloys: (i) a decrease in density, (ii) an increase of the elastic modulus, and (iii) an increase in strength. In order to achieve a significant room-temperature strength contribution from the beryllium dispersoids, it would be necessary to avoid excessive coarsening of them during metallurgical processing. However, it has been shown [3, 4] that Al–Be binary alloys (containing up to 10 wt % Be) produced by RSP have a fine dispersion of α-Be particles. Upon subsequent heat treatment the particles coarsen somewhat but remain with average sizes smaller than 100 nm.

In RSP aluminium alloys containing both lithium and beryllium, two different precipitates form independently [1]. The Al_3Li (δ') phase precipitates as fine, coherent spheroids which will provide a significant contribution to strength [5, 6]. The α-Be precipitates as a dispersoid within the aluminium matrix. It is anticipated that this α-Be could contribute to the mechanical properties of the alloy by adding a dispersion-strengthening component to the yield strength, and also by providing a mechanism to disperse dislocation glide, which will allow the Al_3Li phase to contribute more of its full potential to the alloy strength. It has been shown that very fine dispersoids provide a beneficial effect on improving the dispersion of slip in Al–Li alloys [6]. Because the Al_3Li (δ') coherent precipitates are small (2 to 100 nm, depending upon ageing conditions) and their misfit with the aluminium lattice is small (less than 0.1%), they are readily sheared by dislocations and slip can occur by planar glide in Al–Li alloys containing more than about 1 wt % Li. Both the limited ductility and low fracture toughness of various Al–Li alloys have been broadly attributed to this planar glide mechanism [6]. There are no known intermetallic compounds between lithium and beryllium [7] and so it is reasonable to expect that these elements will coexist in an alloy without the formation of undesirable phases. The purpose of this paper is to describe recent work on Al–Li–Be ternary alloys containing about 3 wt % Li and up to 20 wt % Be. The structure and properties of alloys after rapid solidification processing will be described.

0022–2461/86 $03.00 + .12

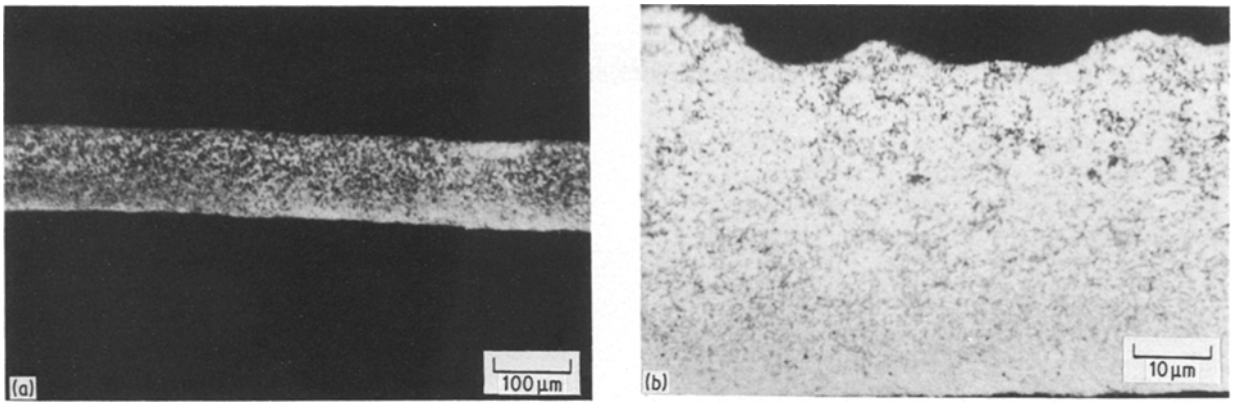

Figure 1 Optical photomicrographs of the melt-spun Al–3Li–10Be alloy (contact surface is the lower surface in each case) at (a) low and (b) high magnifications in the etched condition.

2. Experimental procedure

Two alloys (Al–3Li–2Be and Al–3Li–10Be by wt %) were converted to melt-spun ribbon using equipment designed and built at the Lockheed Palo Alto Research Laboratory [1]. Ribbon of approximate dimensions 1 to 2 mm in width and 20 to 70 μm thickness was produced. The ribbon was examined using optical and transmission electron microscopy. For consolidation, the ribbon was comminuted, cold-compacted to 50 to 60% density, vacuum hot-pressed and extruded [1]. Subsequent heat treatments were carried out in air.

Thinning of the Al–Li–Be alloys for TEM was carried out in an electrolyte of 5% perchloric acid, 35% 2-butoxyethanol and 60% methanol at 10° C with an applied potential of 15 V and a resultant current of 75 mA. The samples were examined with a JEOL 100CX TEM-STEM at 120 kV.

3. Results and discussion

3.1. Melt-spun ribbon

Melt-spun ribbons of Al–3Li–2Be and Al–3Li–10Be alloys were successfully prepared by melt spinning. Optical photomicrographs of melt-spun ribbon of the Al–3Li–10Be alloy are shown in Fig. 1. As may be

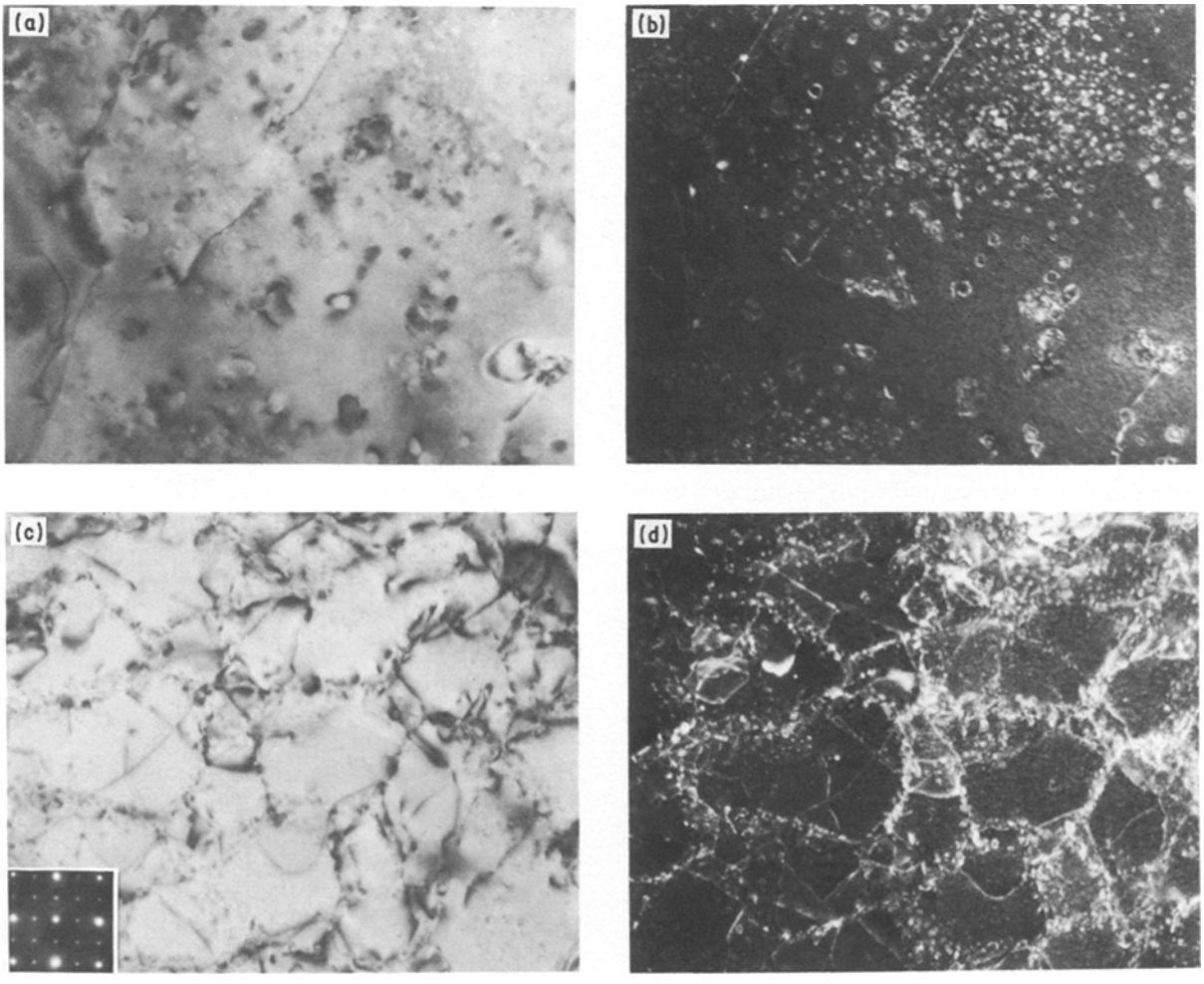

Figure 2 (a) Bright-field and (b) weak-beam dark field of Al–3Li–2Be ribbon. (c) Bright field and (d) weak-beam dark field of Al–3Li–10Be ribbon with inserted [0 0 1] diffraction pattern showing δ' reflection.

seen, relatively uniform microstructures are observed using optical microscopy. These fine structures can be compared with those produced by splat quenching of the same alloy [8] and it is evident that the melt-spinning operation produces a more uniform, finer structure than does the splat quenching.

In order to examine the microstructures of the ribbons more closely, a TEM examination was carried out.

Figs 2a and b show a bright-field/weak-beam dark-field (BF/WBDF) pair showing a typical microstructure of an as-quenched Al–3Li–2Be alloy. The prominent features of this structure are indicated on the micrographs, and include coherent Al_3Li δ' precipitates, and large and small α-Be particles; some regions of cellular structure are also observed. This non-uniform microstructure is similar to that of splat-quenched Al–Be alloys [8]. The δ' particles are approximately 5 to 10 nm in diameter, which is similar in size to δ' observed in as-quenched Al–Li base alloys produced by powder metallurgy or ingot metallurgy techniques. The volume fraction of large (> 100 nm) α-Be particles is relatively low (< 0.10) and these particles are usually confined to grain-boundary regions.

The striking feature evident in the micrographs in Figs 2c and d is the segregated cellular structure of the as-quenched Al–3Li–10Be ribbon. There is an enrichment of small α-Be particles concentrated at the cell walls. Although it is not obvious from these figures the volume fraction of large α-Be particles is greater in the Al–3Li–10Be alloy than in the Al–3Li–2Be alloy. The inserted ⟨0 0 1⟩ zone axis pattern clearly shows the ⟨1 0 0⟩-type reflections from δ' (identical patterns were obtained from Al–3Li–2Be). These precipitates have the typical cube–cube orientation relationship with the matrix (i.e $[1\,0\,0]_{\delta'}//[1\,0\,0]_{Al}$, $(0\,0\,1)_{\delta'}//(0\,0\,1)_{Al}$).

The selected-area diffraction technique was not sensitive enough to reveal the crystal structure of the α-Be particles; therefore, microdiffraction techniques were employed for this purpose. Analyses of particles of about 200 nm were carried out using convergent beam microdiffraction patterns formed by focusing a 100 nm probe (convergence angle = 1.5 mrad) on the precipitate. The reflection from the precipitates confirmed that they are primary α-Be and are randomly oriented within the grains, indicating that they formed prior to the solidification of the aluminium matrix. This is also commonly observed in splat-quenched hypereutectic Al–Be alloys [9].

Similar microstructures have been observed recently in rapidly-solidified Al–Be binaries [10, 11]. Van Aken and Fraser [10] ascribe the morphology and distribution of the α-Be particles to a monotectic reaction. Their proposed solidification scheme requires liquid-phase separation within a metastable miscibility gap. Tanner *et al.* [11] have suggested that α-Be precipitation is due to a simple eutectic reaction similar to the Cu–O and Fe–MnS systems. More detailed experimentation is necessary to determine the exact nature of the phase transformation.

3.2. Consolidated and heat-treated ribbon

Ribbons of both the Al–3Li–2Be and Al–3Li–10Be alloys were converted into extruded bar using techniques previously described [1]. Tensile samples were fabricated from these bars, heat treated to an approximately peak-strength condition and then tensile tested.

It was shown previously that both Al–3Li–2Be and Al–3Li–10Be alloys exhibited age-hardening responses upon ageing at 190° C after quenching from 538° C [1]. The hardening response is representative of the precipitation of Al_3Li (δ') [5, 6]. For example, in the as-quenched condition the Rockwell hardness R_B is 16.5; after ageing at 190° C for 22 h, R_B is 74 [1].

Similar results were observed for an Al–3.6Li–9.8Be alloy [1]. This alloy also was tensile tested and has a modulus of 93.4 GPa, a yield strength of 427 MPa, ultimate tensile strength of 500 MPa and 5.6% elongation. The relatively low strain to failure was traced to inhomogeneities that appear as coarse particles on the fracture surface.

In the following subsection a TEM study of these alloys in the peak-strength condition is presented. Following this, a study of the alloys after tensile testing is described. In both cases, TEM samples were taken such that the thin foil lay parallel to the original extrusion direction. In general, coarsening of the α-Be particles from a size of less than 100 nm in the as-quenched melt-spun ribbon to the size range of 100 to 500 nm in the final product was observed to have taken place as a result of consolidation.

3.2.1. Al–3Li–2Be

Rather inhomogeneous structures were observed in these samples. For example, in Figs 3 and 4, TEM collages from adjacent regions within the same sample are shown. In Fig. 3 there is no elongated grain structure as is evident in Fig. 4. (As will be seen, such regions do not occur in the Al–3Li–10Be alloy, possibly due to the presence of a much greater volume fraction of α-Be particles.) Furthermore, in both Figs 3 and 4 there appear to be intense deformation zones (the black areas in Fig. 3 are regions of high defect density) associated with the α-Be particles. A high-magnification bright field/dark field (BF/DF) pair (using a δ' reflection) is shown in Fig. 5. The α-Be particles do not appear using this reflection but their location can be inferred by the absence or low density of δ' in these regions. The δ' particles are about 20 to 50 nm in size (by comparison, particles of 5 to 10 nm are observed in the as-quenched melt-spun ribbon).

3.2.2. Al–3Li–10Be

In this alloy, the grains were generally observed to be elongated with large-angle grain boundaries along the longitudinal axis and generally small-angle boundaries perpendicular to them. An example is shown in the TEM collage of Fig. 6. The large volume fraction of α-Be particles is also evident. These particles are both on grain boundaries and within grains and have, in some cases, particular orientation relationships with the matrix, e.g. $(1\,0\,\bar{1}\,0)_{Be}//(0\,0\,2)_{Al}$. A region from within the overview microstructure of Fig. 6 is shown in Figs 7 and 8, at low and high magnifications, respectively. In addition to the large α-Be particles (left hand side of Fig. 7), some agglomeration of the smaller

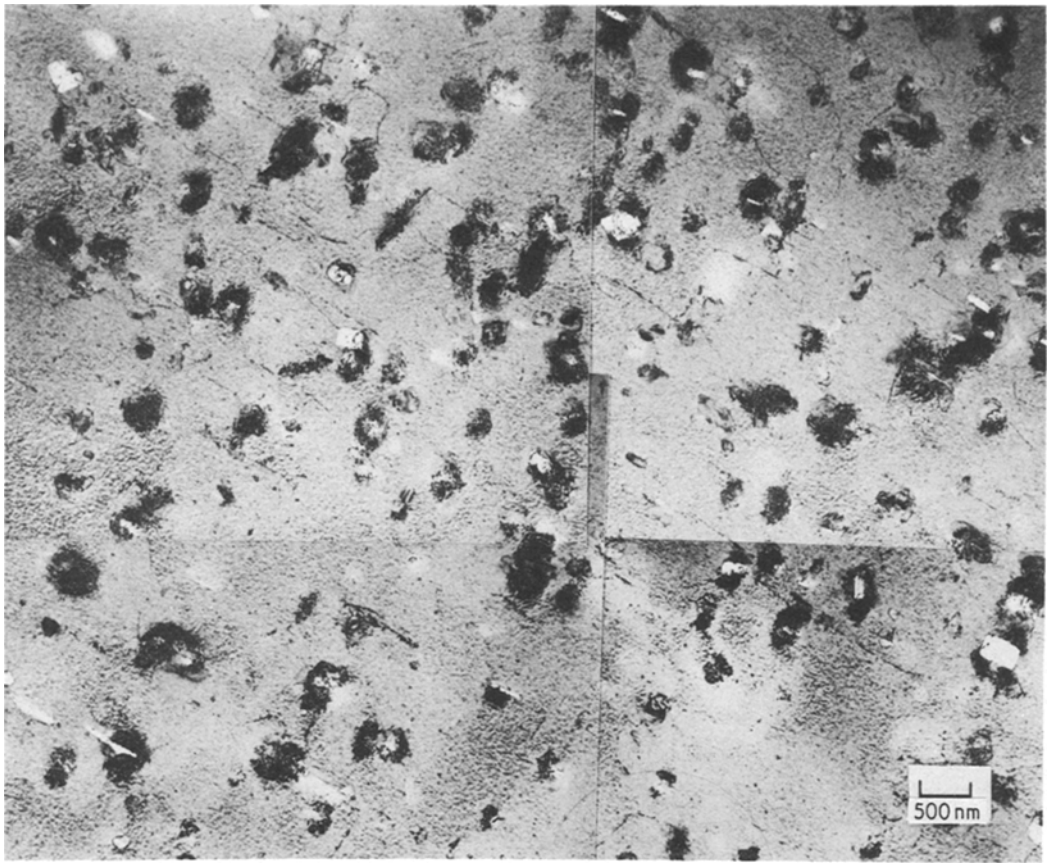

Figure 3 Consolidated ribbon of Al–3Li–10Be alloy, extruded and heat-treated to the T6 condition. This region shows a single crystal containing α-Be particles associated with intense deformation zones.

beryllium particles has occurred during the consolidation processing. This is clearly seen in Fig. 8 in a region adjacent to a boundary.

3.3. Consolidated, heat-treated and tensile-tested condition

The above samples were also examined in the gauge length of tensile coupons after mechanical testing. As expected, the major difference between the samples in the as-heat-treated condition and those in the heat-treated and strained condition is the increased dislocation density. The visibility of the dislocations depends, of course, on the diffraction conditions of the particular region. There was no clear indication of

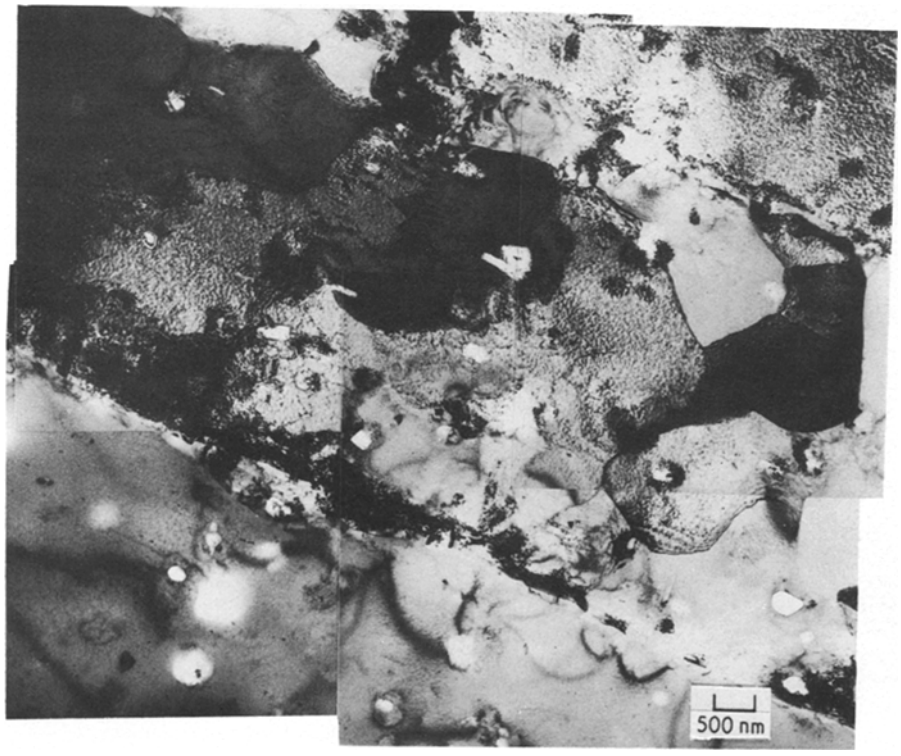

Figure 4 Consolidated ribbon of Al–3Li–2Be alloy, extruded and heat-treated to the T6 condition, but from a nearby region to that in Fig. 3. In this case, elongated grains and subgrains are observed in addition to α-Be particles and deformation zones.

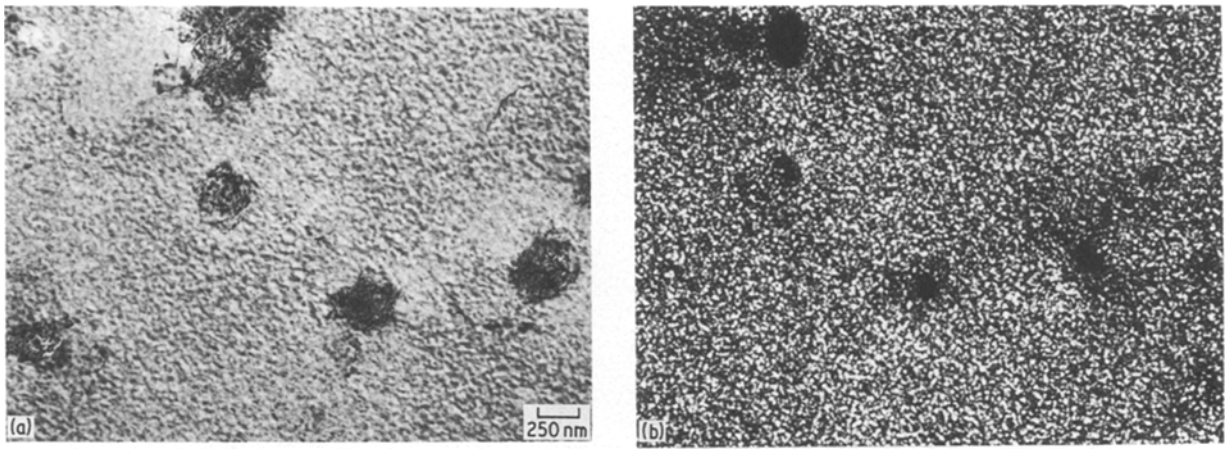

Figure 5 (a, b) BF/DF (δ' reflection) pair of TEMs from the Al–3Li–2Be consolidated ribbon in both the extruded and heat-treated to T6 conditions.

interactions between the dislocations and particles (α-Be or δ') in the samples examined in this study.

For the Al–3Li–2Be alloy in the aged condition, the grains are not elongated. There are large grains with isolated regions containing smaller subgrains as shown in Fig. 9 and there are large depleted zones at the grain boundaries (i.e. regions devoid of δ' particles). Again, the α-Be has mainly precipitated at the grain boundaries of these smaller grains, and is dispersed throughout the larger grains. The precipitate-free zones are particularly evident in the BF/DF pair of Fig. 10 (using a δ' reflection). At present, there is no clear reason why there are the δ'-depleted zones within the grains. Some of these regions could be sites for α-Be dispersoids but not all of them can be.

For the case of the Al–3Li–10Be alloy in the peak-aged and tensile-tested condition, there are many beryllium particles as shown in Fig. 11. The large α-Be particle in Fig. 12 is of particular interest. The small precipitates on the α-Be particle could be small α-Be particles. This type of precipitate has previously been observed by Van Aken and Fraser [10] and by Tanner [4] in Al–Be binary alloys. The convergent-beam electron diffraction pattern in Fig. 12 is typical for this precipitate.

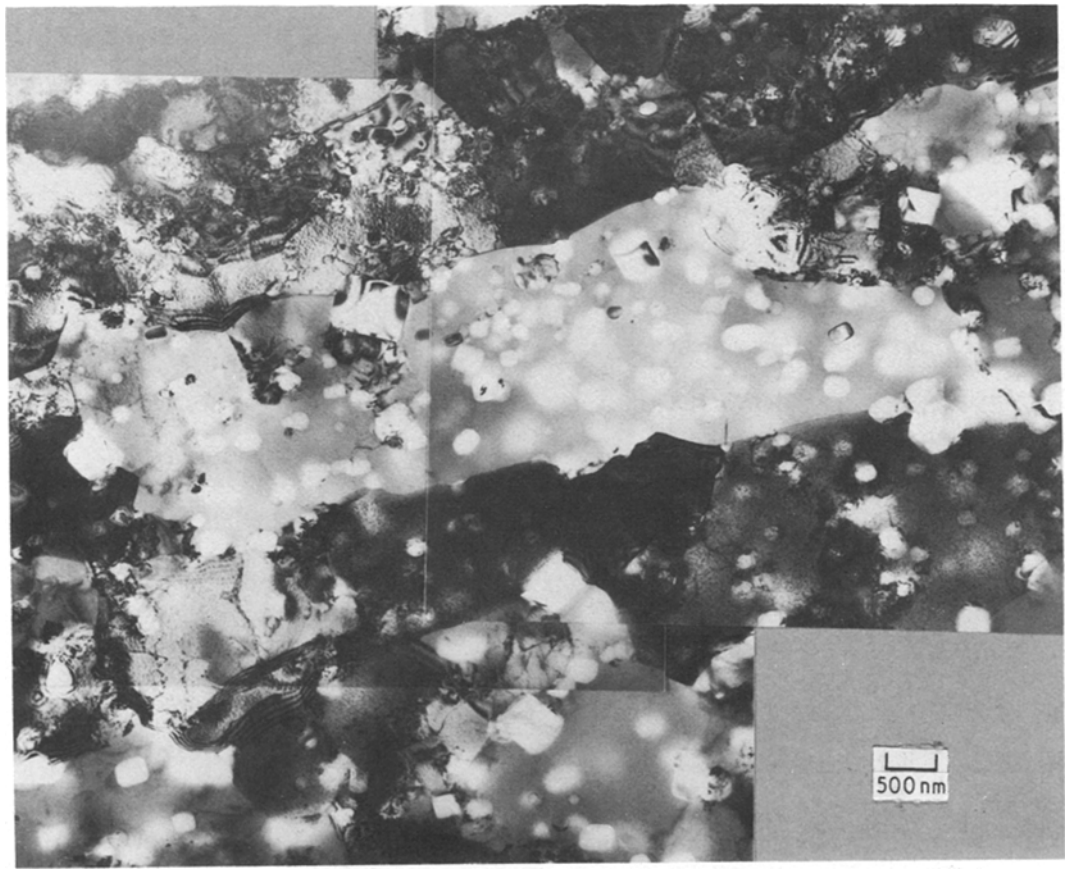

Figure 6 TEM collage of the Al–3Li–10Be consolidated melt-spun ribbon in the extruded plus T6 heat-treatment condition.

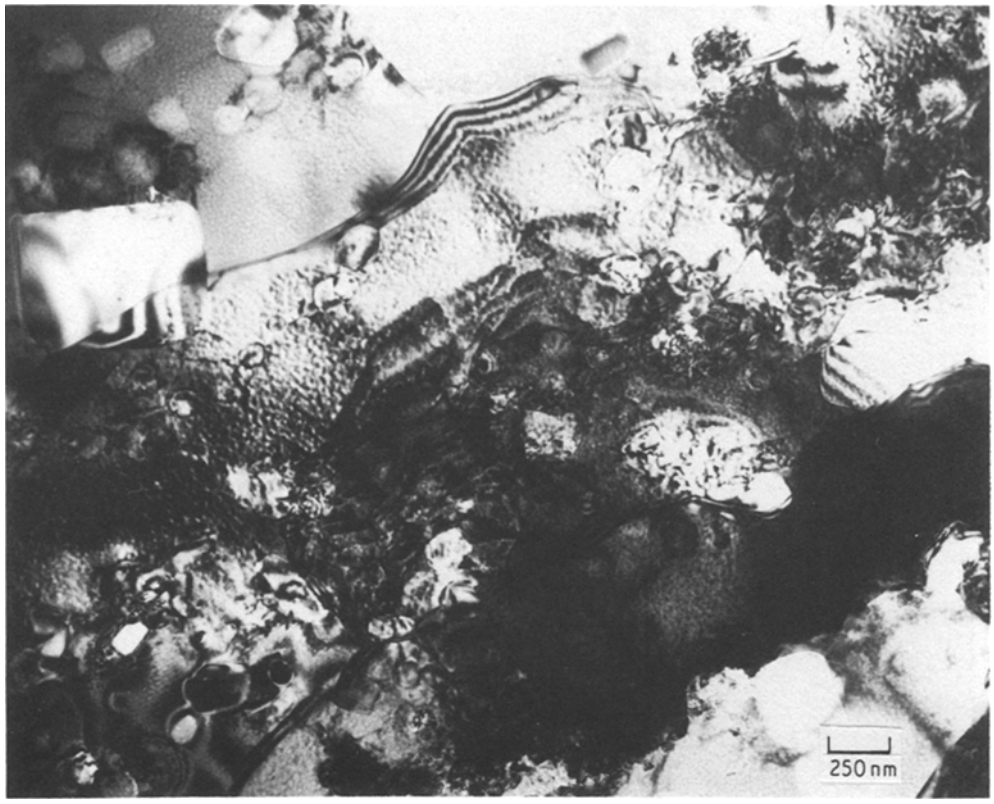

Figure 7 Consolidated and heat-treated Al–3Li–10Be alloy.

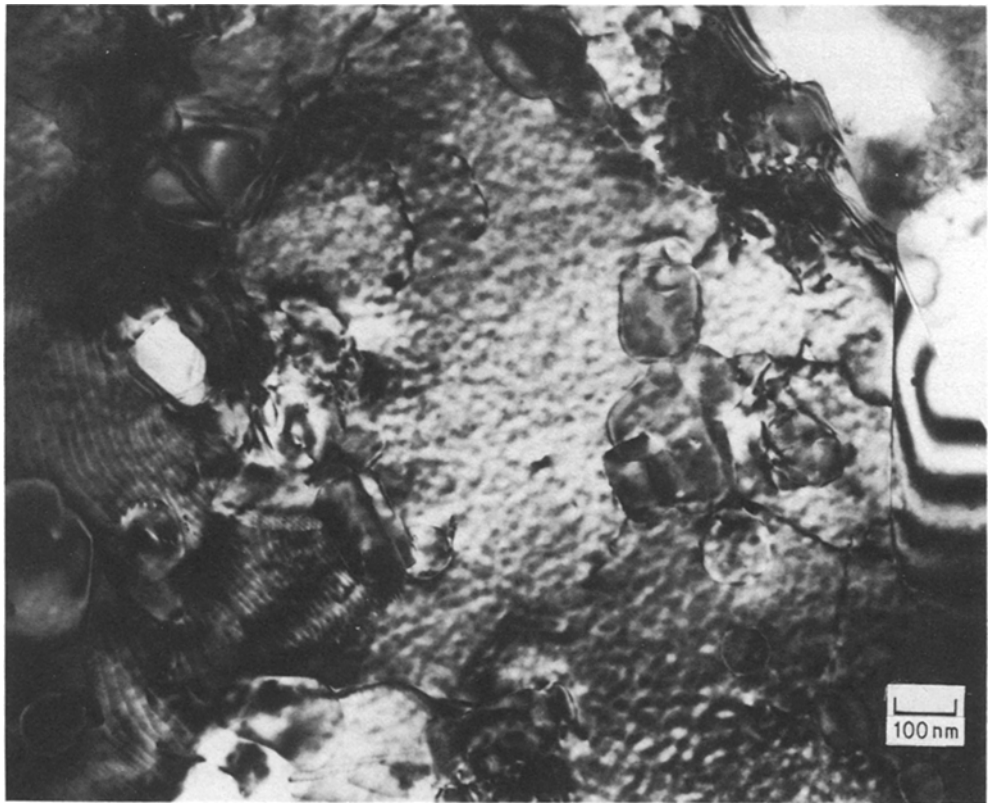

Figure 8 Region from within Fig. 7 showing agglomeration of small beryllium particles as a result of consolidation.

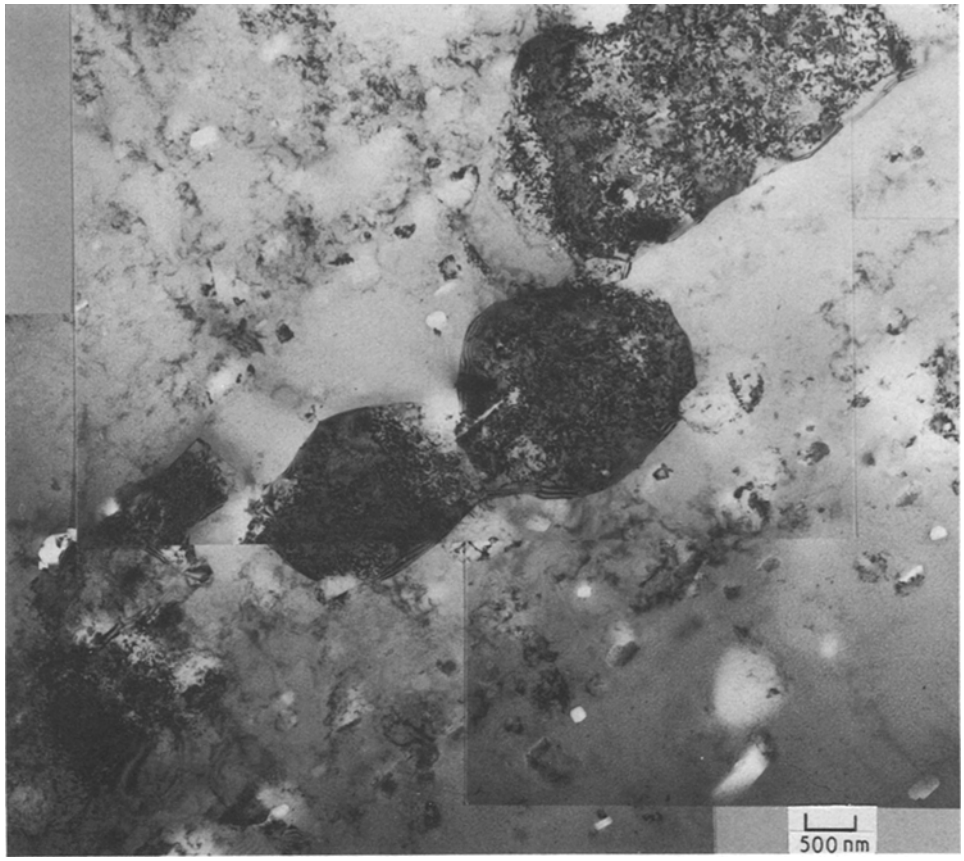

Figure 9 Consolidated Al–3Li–2Be after tensile testing.

4. Summary

Two low-density, high-modulus aluminium–lithium–beryllium alloys (Al–3Li–2Be and Al–3Li–10Be by wt %) have been produced by rapid solidification via melt-spinning. The alloys have been consolidated, heat-treated to maximum strength and tensile-tested. The mechanical properties of the alloys in the heat-treated condition have been described. The microstructures of the alloys in each of the above conditions have been investigated using transmission electron microscopy. In the melt-spun condition, the alloys contain fine δ' particles (5 to 10 nm in diameter), some large α-Be particles (> 100 nm), and a segregated dispersion of fine α-Be particles (5 to 50 nm) located on cell boundaries. After consolidation and heat treatment, rather inhomogeneous structures were observed. Coarsening of the δ' and coarsening and agglomeration of the α-Be particles is evident and precipitate-free zones are observed at grain boundaries.

Acknowledgements

This work was supported by the Lockheed Missiles and Space Company, Inc., Independent Research Program and the Office of Naval Research, Contract No. N00014-84-C-0032. The authors wish to acknowledge the contributions of R. M. Harrington of the Lockheed Palo Alto Research Laboratory for the mechanical property test results.

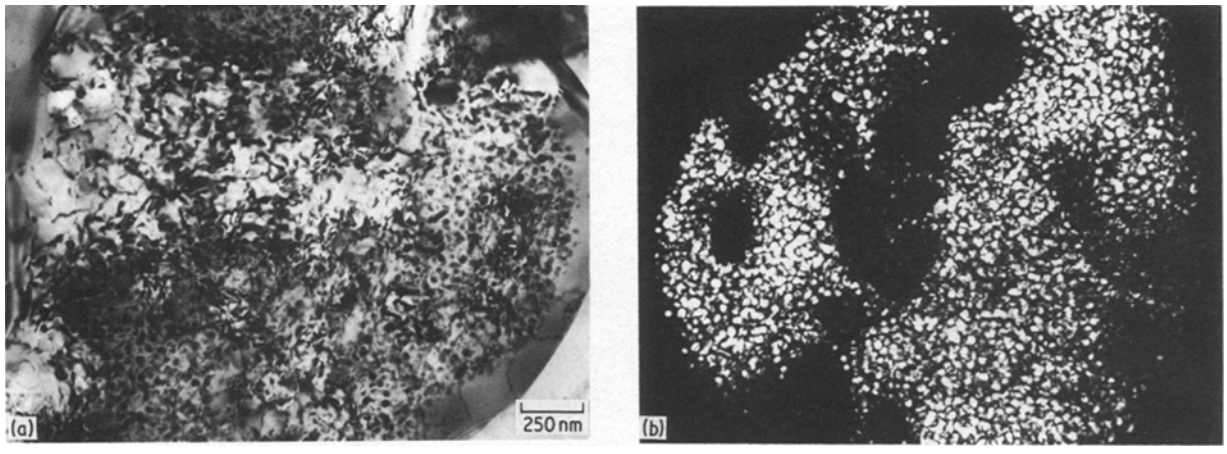

Figure 10 (a, b) BF/DF pair showing depleted region of δ' adjacent to grain boundaries and depleted regions within the grains of tensile-tested Al–3Li–2Be alloy.

Figure 11 Al–3Li–10Be consolidated alloy in the T6 condition after testing.

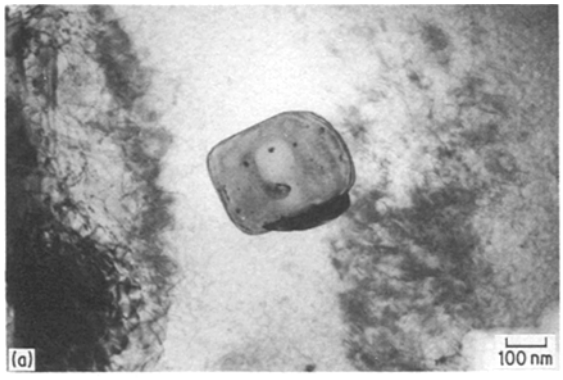

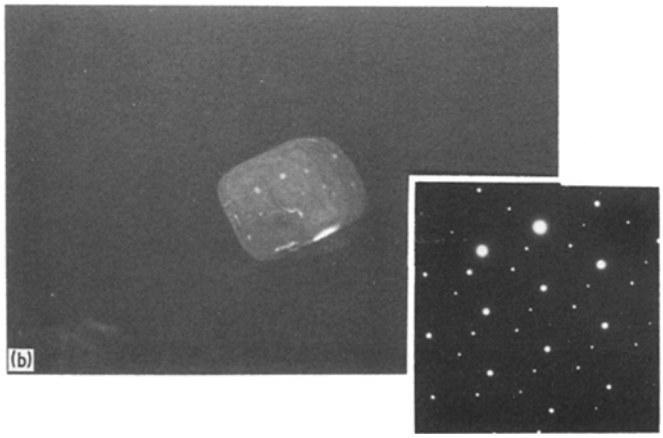

Figure 12 (a, b) BF/WBDF TEM pair showing small beryllium particles on an α-Be particle in the Al–3Li–10Be consolidated alloy. The convergent-beam electron diffraction pattern shown in (b) is typical for this type of precipitation.

References

1. A. E. VIDOZ, D. D. CROOKS, R. E. LEWIS, I. G. PALMER and J. WADSWORTH, in Proceedings of Conference on Rapidly Solidified Powder Aluminium Alloys, ASTM Special Technical Publication No. 890 (American Society for Testing and Materials, Philadelphia).
2. J. WADSWORTH, A. JOSHI, D. D. CROOKS and A. E. VIDOZ, *J. Mater. Sci.* **21** (1986) 3843.
3. A. R. PELTON, F. C. LAABS and J. WADSWORTH, in Proceedings of 21st Annual Electron Microscopy Colloquium, Iowa State University, Ames, Iowa, May 1984, edited by M. C. Thompson, p. 28.
4. L TANNER, private communication (1984).
5. I. G. PALMER, R. E. LEWIS and D. D. CROOKS, in "High Strength Powder Metallurgy Aluminium Alloys", edited by M. J. Koczak and G. J. Hiddeman (Metallurgical Society of AIME, Warrendale, Pennsylvania, 1982) p. 369.
6. E. A. STARKE Jr, T. A. SANDERS Jr and I. G. PALMER, *J. Metals* **33** (8) (1981) 24.
7. R. P. ELLIOT, "Constitution of Binary Alloys", 1st Suppl (McGraw-Hill, New York, 1965) p. 65.
8. J. WADSWORTH, A. R. PELTON and A. E. VIDOZ, *Int. J. Mater. Sci. Eng.*, in press.
9. A. R. PELTON, unpublished work.
10. D. C. VAN AKEN and H. L. FRASER, *Acta Metall.* **33** (1985) 963.
11. L. E. TANNER, L. JACOBSON and R. GRONSKY, in Proceedings of 43rd Annual Meeting of EMSA (San Francisco Press, San Francisco, 1985) p. 50.

Received 19 November 1985
and accepted 10 January 1986